ELSEVIER

Thin Solid Films 00 (2001) 00–00

thin solid films

www.elsevier.com/locate/tsf

# Evidence of a high density of fixed negative charges in an insulation layer compound on silicon

D. König[a,*], M. Rennau[b], M. Henker[b], G. Ebest[a]

[a] *Faculty of Electrical Engineering, Technical University of Chemnitz, 09107 Chemnitz, Germany*
[b] *Centre of Microelectronics, Technical University of Chemnitz, 09107 Chemnitz, Germany*

Received 19 November 1999; received in revised form 31 October 2000; accepted 7 December 2000



**Abstract**

For drift field generation, IS structures with a positive interface charge in an insulator compound were developed in the 1980s and employed mainly on field effect solar cells. While there has been a large number of publications about the positively biased insulator–semiconductor structure there has been very little interest in its antipolar counterpart — the negatively biased insulator–semiconductor structure — so far. However, by using that structure as a second drift field source for field effect solar cells their conversion efficiency could be improved. The conventional rear surface passivation of silicon active layers by shallow ultrahigh aluminium doping in order to form a back surface field involves a high density of lattice and surface defects which increase recombination rates. The structure introduced herein is put onto a silicon layer and acts thus as an external negative drift field source, thereby avoiding the drawbacks of ultrahigh doping. The layer arrangement aluminiumfluoride–silicon dioxide on silicon seems to be a good candidate for a negative drift field source. Experimental results which led to a fixed interface charge of up to $-1.6\times10^{12}$ cm$^{-2}$ at the interface aluminiumfluoride ‖ silicon dioxide are presented and an interpretation of the fixed negative charge is given. 

*Keywords:* Surface and interface states; Field effect; Silicon; Solar cells

## 1. Introduction

Insulator–semiconductor (IS) structures are widely used in electronic devices. Normally one strives for a minimum interface charge density as it shifts the flat band voltage towards zero bias over the IS structure, resulting in improved sensibility of active semiconductor devices like metal oxide semiconductor field effect transistors (MOSFETs). On the other hand, there are important applications of positively biased IS structures as in field effect solar cells [1].

While this positively charged IS structure is employed on an industrial scale for producing metal insulator semiconductor (MIS) solar cells it seems that only one work [2] had been published concerning a negatively charged IS structure. However, employing a negative drift field source to the rear surface of MIS solar cells could replace the conventional back surface field (BSF) produced by shallow thermal diffusion of aluminum (Al) into the silicon (Si) layer.

In this paper first experimental results of an IS structure with a high density of negative interface charges — called $I^-S$ structure — consisting of aluminiumfluoride ($AlF_3$) and silicon dioxide ($SiO_2$) are presented. We think that the replacement of the BSF source according to [3] will improve device efficiency for a number of reasons as briefly outlined below. Section 2 describes the preparation of the $I^-S$ structures. In Section 3 the employed measurement

* Corresponding author. Tel.: +49-371-531-3089; fax: +49-371-531-3004.
*E-mail address:* dirk.koenig@e-technik.tu-chemnitz.de (D. König).

0040-6090/01/$ - see front matter 
PII: S0040-6090(01)01926-X

processes are described. Section 4 presents the measured data. The phenomenon of strong electron localization at the interface ($\|$) $AlF_3 \| SiO_2$ is discussed in Section 5. A conclusion from experimental results and theoretical considerations is drawn in Section 6.

The preparation of the BSF at Si solar cells is done by rapid thermal diffusion (RTD) of Al into the p-Si substrate. Improvement of efficiency thereby is evident, but owing to ultra high doping there are several draw backs:

1. At high doping levels, bulk and surface defect density rise tremendously due to a perturbed Si lattice. Thermally inactive dopants at interstitial sites and stretched/tilted/broken bonds lead to a much increased bulk and surface recombination rate at the rear surface.
2. The field strength from a $p^+$ layer at the rear surface is significantly lower compared to a layer system with a high negative charge as an external drift field source [4] which is especially valid for carrier separation at significant currents (e.g. near the Maximum Power Point, MPP). Then the screening of the negative charge is incomplete due to continuous recombination of attracted holes with injected electrons from the rear contact, leading to an increased total drift field within the bulk as both fixed antipolar charges add up their field strength.
3. If a BSF is created by RTD a proper surface passivation of Si is difficult due to the high doping density at the rear surface.
4. When insulation layers are used for the $I^-S$ structure the cell can also be illuminated from the rear surface because it consists of isolators which are transparent for wavelengths $\lambda \geq 200$ nm. Thus an increased blue response at the rear surface can be expected.
5. If the insulation layers are carefully designed such that $n_{iso} \cdot d_{iso} = \lambda_{sun}/4$ they can work simultaneously as anti-reflective coating (ARC) at bifacial solar cells or — in case of a monofacial solar cell — can provide a good back surface mirror.

All drawbacks mentioned above have an increasing deteriorating effect on device efficiency with decreasing Si substrate thickness. So by creating an $I^-S$ structure at the rear surface device efficiency can be improved significantly which becomes especially useful for thin substrates and films [5]. Another supporting fact is that solar cell manufacturers are striving for thin active layers for obvious reasons not further discussed here.

## 2. Sample preparation

Boron doped crystalline Si ($\langle 100 \rangle$ c-Si, $10^{16}$ $cm^{-3}$) wafers were thermally oxidized at 1000°C for 360/160 s in an ambient $HCl/O_2 = 3/97$ so that a thermal $SiO_2$ layer of a thickness $d_{SiO_2} = 20$ nm/10 nm was formed. Upon these $SiO_2$ layers $AlF_3$ was deposited at 250°C in high vacuum to a thickness of $d_{AlF_3} = 120$ nm. One wafer with $d_{SiO_2} = 10$ nm was prepared without $AlF_3$ deposition in order to serve as a reference. All samples were stored in air at room temperature after preparation.

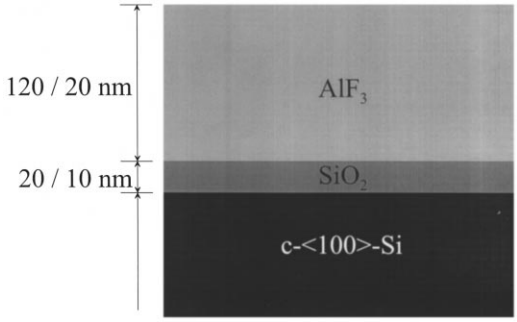


Fig. 1. Physical structure of the layer arrangement.

Fig. 1 shows the physical structure of the layer arrangement.

## 3. Measurements

The estimation of the respective interface states between the c-Si wafer and the $AlF_3$ layer was realized by the mercury probe capacitance/voltage (Hg-C/V) measurement device SSM 495 from Solid State Measurements. A 50-point wafer map was carried out on all samples. The measurement frequency had been set to 1 Mhz, the active sample area was $2 \times 10^{-2}$ $cm^2$.

The interface charges were calculated from the flat band voltages $V_{fb}$ in respect to $SiO_2 \| Si$. Since the fixed negative charge shall have an impact (i.e. drift field) on the Si layer the effective charge $N_{\| eff}$ of the structure $AlF_3 \| SiO_2 \| Si$ was calculated referring to $SiO_2 \| Si$. Comparable C/V measurements for positively charged $SiO_2$/Si Nitride ($Si_3N_4$) layers (as in [6]) are measured in respect to $SiO_xN_y \| Si$ for the same reason.

Thermal $SiO_2$ layers on c-Si as the ones grown on the samples have an interface trap state density at $SiO_2 \| Si$ of $D_{it\ SiO_2 \| Si} \approx 3\text{–}4 \times 10^{10}$ $cm^{-2}$ [7] which drops to $D_{it\ SiO_2 \| Si} \approx 1 \times 10^{10}$ $cm^{-2}$ if a post oxidation anneal is carried out [8]. The fixed bulk oxide charge of $Q_{SiO_2} = 2.2 \times 10^{11}$ $cm^{-2}$ corresponds well to common values for samples which were not annealed in hydrogen ambient after oxidation [9,10]. $N_{\| eff}$ is the sum of the fixed interface charge at $AlF_3 || SiO_2$, the fixed oxide charge and the interface charge at $SiO_2 || Si$ as a function of their position and the respective dielectric constant $\varepsilon$ of the material which is penetrated by the electric field, referring to $SiO_2 \| Si$. Since all components of $N_{\| eff}$ are considered as charge per square

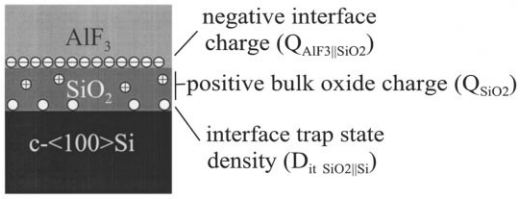


Fig. 2. On the charge of the structure $AlF_3 \| SiO_2 \| Si$.

$[cm^{-2}]$ the fixed oxide charge $Q_{SiO_2}$ has to be divided by $d_{SiO_2}$ which yields the fixed oxide charge per square. For further explanation see also Fig. 2 and Table 1.

Assuming that $Q_{SiO_2}$ and $D_{it\ SiO_2 \| Si}$ is situated at $SiO_2 \| Si$ what is justified for thin $SiO_2$ layers and $Q_{AlF_3 \| SiO_2}$ is situated at $AlF_3 \| SiO_2$ as a first approximation the effective charge density $N_{\| eff}$ is

$$N_{\| eff} = \frac{Q_{SiO_2}}{d_{SiO_2}} + D_{itSiO_2 \| Si} + \frac{Q_{AlF_3 \| SiO_2}}{1 + \frac{d_{SiO_2} \cdot \varepsilon_{AlF_3}}{d_{AlF_3} \cdot \varepsilon_{SiO_2}}} [cm^{-2}]. \quad (1)$$

In order to investigate the time variance (i.e. degradation) of $N_{|| eff}$ Hg-C/V wafermap measurements were carried out on samples 4 and 5 in distinct time intervals.

It is well known that F is a very agile chemical element. In order to preclude that F may falsify the C/V measurements due to diffusion into Si a secondary ion mass spectroscopy (SIMS) measurement was carried out for examining the F content depending on the position within the layer compound.

For obtaining first structural results about the $AlF_3$ layer X-ray-diffraction (XRD)- and X-ray-reflection (XRR) measurements were carried out. The $AlF_3$ layer of a cross-section probe of the $I^-S$ structure was investigated by electron ray diffraction (ERD) for getting further insight into the detailed structure of $AlF_3$, especially near $AlF_3 \| SiO_2$.

## 4. Results

The F profile of the SIMS measurement in Fig. 3 shows that some F penetrates the oxide whereby there is a strong negative gradient within the oxide layer.

There was no F detected within the c-Si. The scattered peaks are due to the fact that during primary ion bombardment ($O^{16}$, $E_{ion} = 10$ keV) of $AlF_3$ gaseous F escapes. For that reason it is subsequently present within the SIMS reactor in concentrations around detection limit.

Table 1 presents Hg-C/V measurement results and corresponding structural data of the samples prepared. All samples have been stored in air at room temperature.

In Fig. 4 the high frequency (HF)-Hg-C/V curves of sample 5 and the reference wafer (sample 6) are shown. They were measured 11 weeks after preparation. The different values for maximum/minimum capacities $C_{max}$, $C_{min}$ are due to the respective total insulation layer thickness.

The Hg-C/V measurements of samples 4 and 5 have been continued over 26 weeks for verifying the stability of $N_{\| eff}$. Fig. 4 shows the time variance of $N_{\| eff}$.

As already supposed in [3] the negative localized states of $AlF_3 \| SiO_2$ dominate the resulting effective interface charge $N_{\| eff}$ towards the Si wafer. Hence, the oxide charge $Q_{SiO_2} \approx 2 \times 10^{11}$ $cm^{-2}$ is completely compensated as it can be seen by comparing the measured values of the samples with the reference (wafer 6).

The values of Table 1 show a clear correlation for the increment of the effective negative interface charge $N_{\| eff}$ with decreasing oxide thickness $d_{SiO_2}$. This is due to the positive bulk charge of $SiO_2$ in compound with the decreasing distance of $AlF_3 \| SiO_2$ from the $SiO_2 \|$ Si. The reference wafer does not possess any fixed negative charges, obviously due to absence of $AlF_3$ on $SiO_2$. Both facts indicate that the negative charge lies at $AlF_3 \| SiO_2$ as already proposed in Section 3.

From Fig. 5 it can be seen that $N_{\| eff}$ even builds up within the first month after preparation, then leveling off at a constant value. So far no degradation of $N_{\| eff}$ occurred.

$AlF_3$ is a material widely used in optics and optoelectronics. It is a pretty rare material for solid state electronics and electrostatics so that basic structural

Table 1
Measurement results and corresponding structural data of the samples prepared, extracted by 50-point wafer maps, after levelling off at constant $N_{\| eff}$ (11 weeks from preparation, see also Figs. 4 and 5); sample 6 (non-annealed $SiO_2$) was added as a reference

| Wafer no. | $d_{SiO2}$ [nm] | $d_{AlF3}$ [nm] | $V_{fb}$ [V] | $V_{thr}$ [V] | $N_{\| eff}$ $\times 10^{11}$ $[cm^{-2}]$ |
|---|---|---|---|---|---|
| 1 | 20 | 120 | 0.50 | 3.22 | −1.7 |
| 2 | 10 | 120 | 0.66 | 3.35 | −2.1 |
| 3 | 1.5 | 120 | 3.76 | 6.86 | −8.6 |
| 4 | 20 | 20 | 1.27 | 2.68 | −11.5 |
| 5 | 10 | 20 | 1.46 | 2.77 | −15.7 |
| 6 | 10 | – | −0.78 | −0.29 | 2.2 |

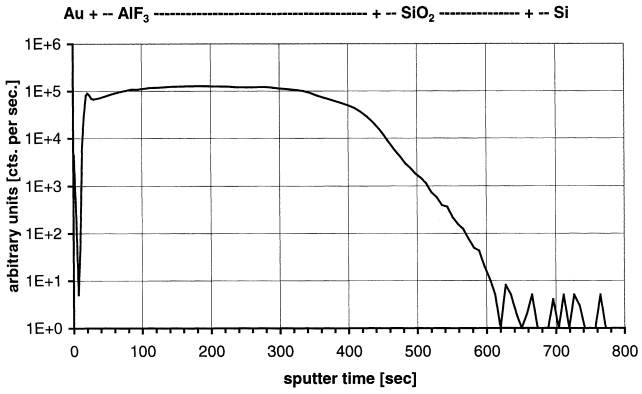


Fig. 3. SIMS profile of the F content within the layer compound; the ultrathin gold layer was deposited onto the sample for draining the charges of the primary ion beam; thickness of layers is not proportional to sputter time due to different sputter rates of materials.

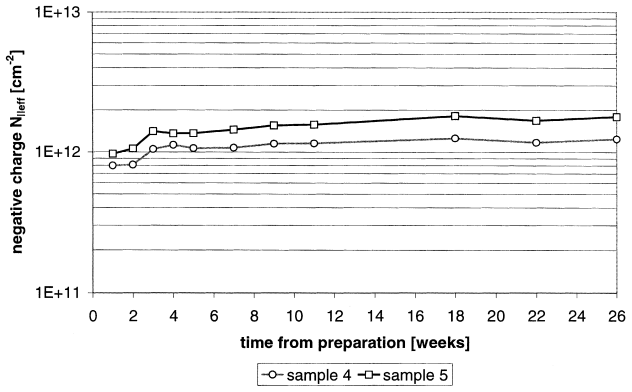


Fig. 5. Negative effective charge $N_{\parallel \mathrm{eff}}$ of samples 4 and 5 as a function of time from preparation (lines are guide to the eye); each point represents the average mean value of a 50-point Hg C/V wafermap.

investigations of $AlF_3$ had to be carried out in order to shed some light onto its structural properties and interface formation with $SiO_2$.

Concerning layer orientation and crystallography our X-Ray Reflection (XRR) and X-Ray-Diffraction (XRD) measurements showed that evaporated $AlF_3$ layers are X-ray amorphous. The mass density estimated by XRR was with $\rho_{AlF_3} = 2.8 \pm 0.3$ g cm$^{-3}$ lower than expected. The very smooth surface of the $AlF_3$ film estimated by XRR also shows that it is X-ray amorphous. XRR with high energy coherent X-rays could reveal nanocrystalline structures within the range of up to 50 Å [11].

Better structural results emerged from low energy electron ray diffraction (ERD) measurements of a cross-section probe, whereby $AlF_3$ near the interface $AlF_3 \parallel SiO_2$ was investigated. $AlF_3$ is known to recrystallize under a high energy electron beam [12] so that the energy range of the electrons had to be chosen with care. At an online observation of the ERD image no recrystallization (i.e. emergence of new rings/spots) was noticed. Fig. 6 shows the ERD image of sample 3.

From Fig. 6 it can be seen that the general structure of $AlF_3$ is amorphous. There are several bright spots which indicate the presence of highly oriented crystalline areas. A faint ring can be seen at a space angle position which corresponds to the hexagonal orientation of $AlF_3$ base cells.

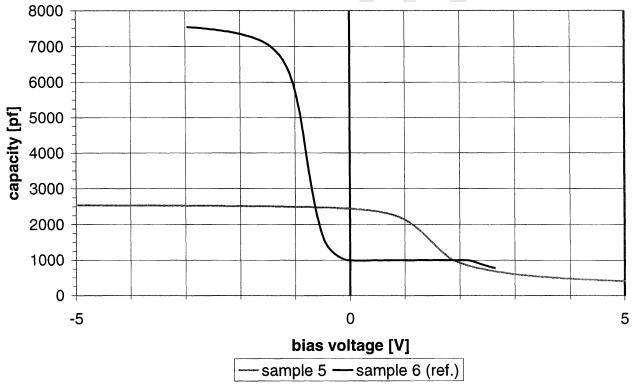


Fig. 4. HF–Hg–C/V curves of samples 5 and reference sample 6, measured 11 weeks after preparation; different values for $C_{\max}$, $C_{\min}$ are due to the respective total insulation layer thickness.

## 5. Discussion

The mechanism of massive electron localization at the interface $AlF_3 || SiO_2$ is not quite clear yet. The presence of F vacancies at $AlF_3 \parallel SiO_2$ seems to play a key role for the localization of electrons.

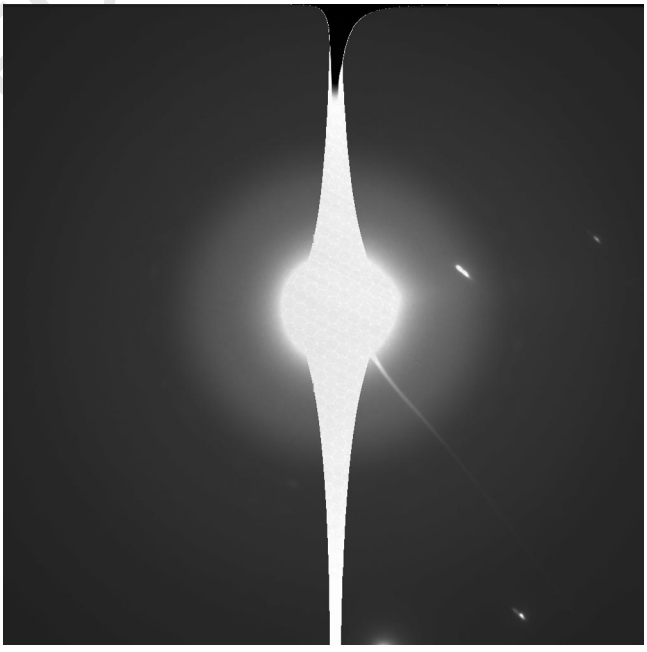

Fig. 6. Low energy ERD image of the $AlF_3$ layer (cross-section probe, sample 3) near the interface $AlF_3 \parallel SiO_2$. The bright spots indicate the presence of highly oriented crystallite areas within the amorphous $AlF_3$ matrix. A faint ring can be seen at a space angle position which corresponds to the hexagonal orientation of $AlF_3$ base cell clusters.

When depositing $AlF_3$ films by evaporation the stoichiometric ratio of Al/F — 1:3 is not reached [13]; such $AlF_3$ layers consist actually of $AlF_x$ with $x \approx 2.6–2.9$. An imbalanced ratio Al/F appears to have a very strong influence on the density of localized negative charges at F vacancies as well.

A possibility for occupying the 2p6 electron state of the F cores could be provided by electrons from Si tunnelling through $SiO_2$ to $AlF_x$. The 2p6 electron state of F lies very deep within the valence band so that they are strongly localized there; for that reason further movement under excitation with sunlight is not possible. Thus, the increase of $N_{\parallel \mathrm{eff}}$ within the first 4 weeks after preparation could originate from Si electrons tunnelling through $SiO_2$ to very deep localized states with an extremely low tunnelling probability. For that reason the occupation of the 2p6 states takes quite a long time. The driving force for tunnelling is apparently the Coulomb force of unoccupied F vacancies near or at $AlF_x \parallel SiO_2$. Therefore, a strongly localized negative interface charge could consist of a surplus negative charge at F vacancies at $AlF_3 \parallel SiO_2$.

An effect which has to be taken into consideration at $AlF_3 \parallel SiO_2$ is the exchange of O and F between $AlF_3$ and $SiO_2$ according to the F profile of the SIMS measurement. As reported in [14], F Atoms can react with O, Al and Si to chemical compounds of the form $AlO_xF_y$ and $SiO_xF_y$.

It was mentioned in Section 4 that the density of the $AlF_3$ film was estimated to be $\rho_{AlF_3} = 2.8 \pm 0.3$ g cm$^{-3}$. This value gave a clue about the composition in respect to the orientation of different basis sets of unit cells as an amorphous structure with crystallites with extensions up to 50 Å is expected [11]. There are three different phases of $AlF_3$:

- Hexagonal $\rho_{AlF_3} = 2.815$ g cm$^{-3}$ [15]
- Rhombohedral $\rho_{AlF_3} = 3.192$ g cm$^{-3}$ [16]
- Tetragonal $\rho_{AlF_3} = 3.016$ g cm$^{-3}$ [17]

Probably the manufactured $AlF_3$ layers are dominated by hexagonally orientated unit cells. Rhombohedrally orientated unit cells do not seem to occur.

While there are quite a number of publications about atomistic material descriptions of the bulk phases of Fluorides, e.g. [18–20], there are only few dealing with the same issue for triple metal-fluoride compounds like crystalline $AlF_3$ [21]. They do not correspond to the deposited $AlF_3$ layers as they are X-ray amorphous as already stated in Section 4. However, no papers which deal with modelling of $AlF_3 \parallel SiO_2$ on an atomistic scale were published so far. Since the phenomena of the structure $AlF_3 \parallel SiO_2 \parallel$ p-Si were discovered by the authors very recently, there is no quantitative model in existence yet. The potential general ground state [22] and exited state models [23] will have to be adapted to the strong ionic nature of $AlF_3 \parallel SiO_2$, especially in respect to hopping interaction and electron confinement [24]. A promising method for modelling both amorphous $AlF_3$ bulk and surface was introduced in [25].

Detailed characterization on an femtoscopic scale and atomistic modelling of $AlF_3$ bulk phases and surfaces towards $SiO_2$ are necessary for providing detailed insight into the working principle of the I$^-$S structures manufactured.

## 6. Conclusions

I$^-$S structures consisting of $AlF_3 \parallel SiO_2 \parallel$ p⟨100⟩Si were manufactured, their total fixed interface charge was measured and first $AlF_3$ film and interface characterizations were carried out.

The average value of the effective fixed charge over the whole layer arrangement $N_{\parallel \mathrm{eff}}$ was estimated by Hg-C/V measurement to $-0.2$ to $-1.6 \times 10^{12}$ cm$^{-2}$ with decreasing oxide thickness, including the compensated positive oxide charge. Two samples were measured over a period of 26 weeks. No degradation of the negative charge occurred so far. The $AlF_3$ layer was found to be X-ray amorphous and seems to consist mainly of hexagonally orientated $AlF_3$ unit cells with some tetragonally orientated unit cells incorporated. ERD investigations confirmed the X-ray amorphous structure and revealed that there are small but highly oriented crystallite areas within the $AlF_3$ layer. A slightly preferred hexagonal orientation of $AlF_3$ base cells within the amorphous layer matrix was detected.

The structure introduced is the first of its kind which is able to localize such a large quantity of negative states at an interface between two insulation layers.

The considerations about the I$^-$S structure presented are merely a first attempt to understand the phenomena observed. Much research work still has to be done in order to describe these layer arrangements in more detail and develop a detailed quantitative model.

## Acknowledgements

The author would like to thank J. Heber, FHI für angewandte Optik und Feinmechanik, Abteilg. Optische Schichten in Jena for the preparation of $AlF_3$ layers and R. Scholz, Institute of Physics, TU Chemnitz, for fruitful discussions.

## References

[1] M.A. Green, A.W. Blakers, J. Shi, E.M. Keller, S.R. Wenham, IEEE Tr. Electron. Devices 31 (1984) 679.
[2] K. Jäger, R. Hezel, A Novel Thin Silicon Solar Cell With $Al_2O_3$ As Surface Passivation, Proc. of the 18th IEEE PVSC, Las Vegas, 1985, p. 1752.

[3] D. König, G. Ebest, Solid State Electron. 44 (2000) 111.
[4] K.W. Böer, Survey of Semiconductor Physics, Vol. 2, Van Nostrand Reinhold, New York, 1992, chapter 23.
[5] D. König, G. Ebest, Sol. Energ. Mat. Sol. C. 56 (1998) 67.
[6] K. Jäger, R. Hezel, IEEE Tr. Electron. Devices 32 (1985) 1824.
[7] M. Schulz, Surf. Sci. 132 (1983) 422.
[8] W.D. Eades, R.M. Swanson, J. Appl. Phys. 58 (1985) 4267.
[9] T. Ohmi, M. Masayuki, M. Itano, T. Imaoka, I. Kawanabe, IEEE Tr. Electron. Devices 39 (1992) 537.
[10] H. Fukuda, M. Yasuda, T. Iwabuchi, J. Appl. Phys. 72 (1992) 1906.
[11] W. Heitmann, Thin Solid Films 5 (1970) 61.
[12] G.S. Chen, J. Vac. Sci. Technol. A 17 (1999) 403.
[13] Y. Danto, J. Salardenne, Vacuum 27 (1977) 293.
[14] S.E. Kim, C. Steinbüchel, Solid State Electron. 43 (1999) 1019.
[15] F. Christoph Jr., G. Teufer, US Patent 3 178 483, June 1965.
[16] E. Staritzky, L.B. Asprey, Anal. Chem. 29 (1957) 984.
[17] D.B. Shinn, D.S. Crocket, H.M. Haendler, Inorg. Chem. 5 (1966) 1927.
[18] R.A. Heaton, C.C. Lin, Phys. Rev. B22 (1980) 3629.
[19] M.A.C. Wevers, J.C. Schön, M. Jansen, J. Phys.: Cond. Mater. 11 (1999) 6487.
[20] H. Tatewaki, Phys. Rev. B 60 (1999) 3777.
[21] P. Daniel, A. Bulou, M. Rosseau, N. Nonet, M. Leblanc, J. Phys.: Cond. Mater. 2 (1990) 5663.
[22] C.M. Goring, R.D. Bowler, E. Hernandez, Rep. Prog. Phys. 60 (1997) 1447.
[23] F. Aryasetiawan, O. Gunnarson, Rep. Prog. Phys. 61 (1998) 237.
[24] M. Schreiber, F. Epperlein, T. Vojta, 23rd Int. Conf. on the Phys. of Semiconductors, Proceedings2, Berlin/Germany, 1996, p. 165.
[25] M. Elstner, D. Porezag, G. Jungnickel, J. Elsner, M. Haugk, Th. Frauenheim, S. Suhai, G. Seifert, Phys. Rev. B 58 (1998) 7260.